CHEMICAL COMPOSITIONS OF MATRICES OF UNEQUILIBRATED ORDINARY CHONDRITES

Yukio IKEDA, Makoto KIMURA,

Department of Earth Sciences, Ibaraki University, Bunkyo 2-chome, Mito 310

Hiroshi MORI and Hiroshi TAKEDA

Mineralogical Institute, Faculty of Science, University of Tokyo, Hongo 7-chome, Bunkyo-ku, Tokyo 113

***Abstract*:** The matrices of six unequilibrated O chondrites and one C chondrite, ALH-764 (LL3), Y-74191 (L3), ALH-77015 (L3), ALH-77033 (L3), ALH-77249 (L3), ALH-77299 (H3) and ALH-77003 (C3), were analyzed and classified into types I and II on the basis of their chemical compositions. The bulk chemical composition of the type I matrix is represented roughly by mixtures of ferrous olivine and sodic plagioclase. The type II matrix resembles the matrices of C2 and C3 chondrites in chemical composition.

1. Introduction

Although the major chemical compositions of bulk chondrules in ordinary chondrites have been reported amply (WALTER, 1969; WALTER and DODD, 1972; MCSWEEN, 1977; DODD, 1978; FODOR and KEIL, 1978), reports on those of matrices are very scarce. Matrices of some unequilibrated ordinary chondrites were analyzed by means of the broad beam electron-probe microanalyzer technique (IKEDA, 1980; HUSS *et al.*, 1981), and were shown to be different in respect to chemical composition from the bulk chondrules. In this paper, the major chemical compositions of matrices of some unequilibrated O chondrites from Antarctica are reported and their origin is discussed.

In general, a "matrix" is considered to be the material filling interstitial spaces between chondrules or large lithic fragments, but the definition of matrix is not strictly given. In this paper, to avoid confusion the matrix of unequilibrated O chondrites is defined as aggregates of materials finer than micron-size. Crystal grains larger than a few microns are classified as mineral fragments (IKEDA, 1980).

2. Description of Matrix

The matrix of ALH-764 chondrite (LL3) is opaque in thin sections (Figs. 1 and 2), but in the thinner periphery of the sections it is a brownish yellow and transparent amorphous material, including crystal grains several to several tens of microns across.

The crystals are troilite, Fe-metal, olivine, and Ca-rich and Ca-poor pyroxenes. These minerals are avoided when the matrix is analyzed by the broad beam electron-probe microanalyzer. The modal volume of the matrix is less than several percent of the whole sample. Detailed petrography and petrology of the chondrite have been presented by IKEDA (1980).

The matrix of Y-74191 chondrite (L3) is reddish brown in color and is a homogeneous amorphous material under microscope (Fig. 3). Sometimes, troilite, Fe-metal, olivine and/or pyroxenes occur in intimate association with the matrix. The matrix modal volume is less than several percent of the whole sample, and detailed petrography and petrology have been reported by IKEDA *et al.* (1979) and KIMURA *et al.* (1979).

The matrix of ALH-77015 chondrite (L3) is observed to be opaque in the thin sections (Fig. 4), but in the thinner periphery of the sections the matrix material is dark brown and amorphous. The matrix is intimately associated with fine grains of troilite, Fe-metal, olivine and pyroxenes. The modal volume of the matrix is less than 1 percent. A brief description is given in Antarctic Meteorite Newsletter by SCORE *et al.* (1981).

A black opaque matrix of ALH-77033 chondrite (L3) occurs around chondrules. It is in intimate contact with patchy troilite. The overall texture of the chondrite resembles that of ALH-77015 chondrite. The modal volume of the matrix is less than a few percent. A brief description of the chondrite is given in Antarctic Meteorite Newsletter by SCORE *et al.* (1981).

A reddish brown matrix of ALH-77249 chondrite (L3) is also made up of amorphous material which surrounds the chondrules and large mineral fragments. In overall texture the chondrite resembles ALH-77015 chondrite. The modal value is less than a few percent. A brief description is given in Antarctic Meteorite Newsletter by SCORE *et al.* (1981).

In ALH-77003 chondrite (C3), small (less than 200 microns) chondrules and fine-grained CAI inclusions are abundant, and the opaque matrix occurs between them (Fig. 5). Tiny grains of troilite and Fe-metal, several to several tens of microns in size, are disseminated throughout the chondrules, fine-grained CAI inclusions and matrix. The modal volume of the matrix may be more than several percent. A brief description is given in SCORE *et al.* (1981) where this chondrite is classified as L3 but may belong to C3.

In ALH-77299 chondrite (H3), chondrules and large lithic fragments are closely packed and interstitial spaces between them are crowded with fine-grained mineral fragments such as olivine, pyroxenes, troilite, Fe-metal and so on (Fig. 6). Areas of the matrix, which were analyzed by using a broad beam (about ten microns) electron-probe microanalyzer, include fine-grained mineral fragments and their finer equivalents. The chemical composition of the matrix is represented by a mixture of "original matrix" and fine-grained mineral fragments.

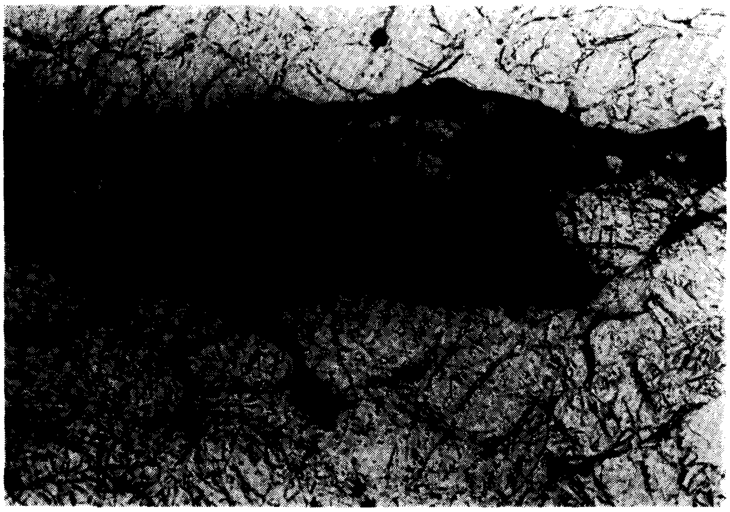

Fig. 1. Matrix of ALH-764 chondrite between two large chondrules (upper and lower), including silicate and opaque mineral grains about several to several tens of microns in size. Long dimension is about 750 microns. Open nicols.

Fig. 2. Dark clast (about 900 × 500 microns in size) and matrix (upper right) around the clast in ALH-764 chondrite. The dark clast resembles the normal matrix under microscope, but the former is slightly darker than the latter, as shown in this figure. Long dimension is about 750 microns. Open nicols.

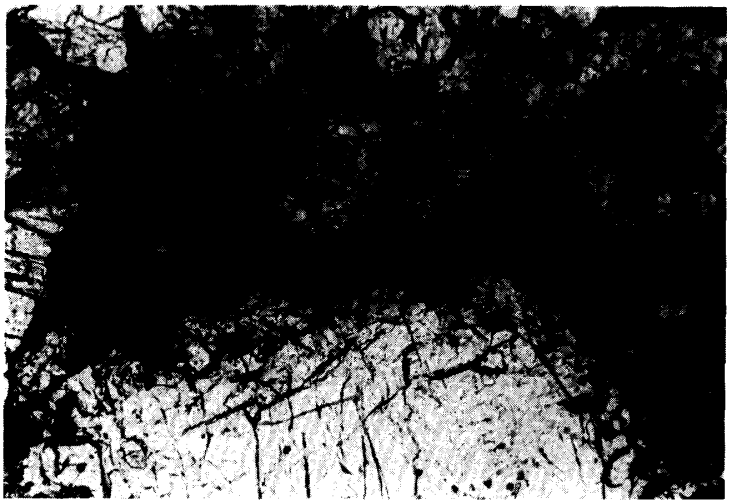

Fig. 3. Matrix of Y-74191 chondrite is shown horizontally in the central part between chondrules. Long dimension is about 750 microns.

Fig. 4. Opaque matrix of ALH-77015 chondrite is shown horizontally in the central part around a large chondrule (lower part). Long dimension is about 750 microns.

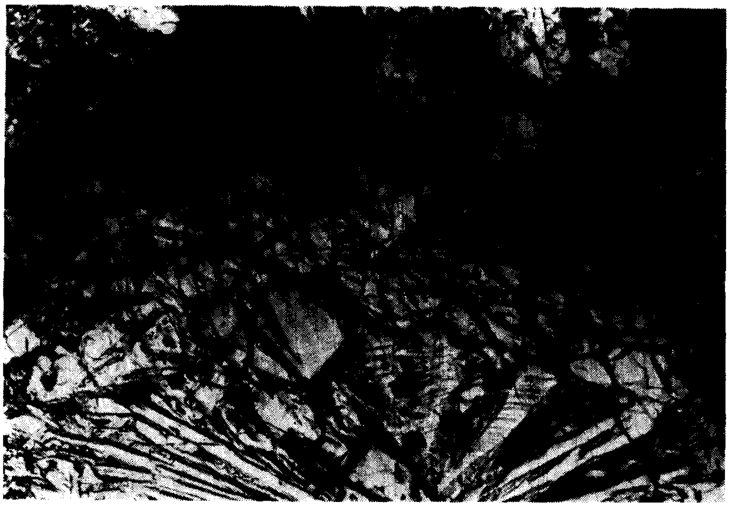

Fig. 5. Matrix of ALH-77003 chondrite around a large chondrule (lower half). Long dimension is 750 microns.

Fig. 6. Matrix of ALH-77299 chondrite is observed in the central part between two large chondrules (upper and lower). It occurs closely with fine mineral fragments of silicate or opaque minerals. Long dimension is about 750 microns.

3. Analytical Method

The matrices were analyzed by two electron-probe microanalyzers, both utilizing a broad beam of about five to ten microns in diameter. The microanalyzers were an ARL-EMX-SM with a take-off angle of 52.5° and an accelerating voltage of 15 kV and a JAX-733 with a take-off angle of 40° and an accelerating voltage of 15 kV. A correction for the occurrence of polyphases in matrices was not applied because analyses of the matrices were performed for the selected areas consisting mainly of submicroscopic fine-grained or amorphous materials. The C and S contents of some matrices were also analyzed for, but no correction is given to these elements in this paper. Thus the C and S contents are shown semiquantitatively in Tables 1, 2, 3 and 8. Total amounts of each oxide of some matrices are far less than 100 wt% and their deficiency may be due to the constituents such as H_2O, P_2O_5, Cl, etc., in addition to C (or CO_2) and S (or SO_2).

A Hitachi H-600 Scanning and Transparent Electron Microscope (STEM) with a Kevex solid state detector was used for the determination of phases of the submicroscopic grains in the matrices.

4. Chemical Composition of Matrices

The chemical compositions of matrices of six unequilibrated ordinary and one carbonaceous chondrites, ALH-764 (LL3), ALH-77015 (L3), Y-74191 (L3), ALH-77033 (L3), ALH-77249 (L3), ALH-77299 (H3) and ALH-77003 (C3) are tabulated in Tables 1 through 7 and are shown in Figs. 7 through 10.

In general, matrices in a chondrite are not very homogeneous in chemical composition. For example, the chemical compositions of matrices of ALH-764 chondrite show a wide variation as seen in the Si-(Mg+Fe)-Al diagram (Fig. 10a), although the ratio of Al-Na-K (Fig. 7a) concentrates in a narrow region. On the contrary, the matrices of some chondrites such as ALH-77015 are homogeneous as shown by the Si-(Mg+Fe)-Al (Fig. 10b) and Si-Mg-Fe (Fig. 9b) diagrams, but show a wide variation in chemical composition as seen in the Al-Na-K diagram (Fig. 7b).

Although the chemical compositions of the matrices vary widely, the variation is not random throughout the chondrite. The matrix around a chondrule shows a rather narrow range and differs systematically from the matrices around other chondrules, but they do overlap in composition with each other. Thus the matrix of a chondrite is characterized by a range of compositions constructed by many analytical points through the chondrite.

The matrices of unequilibrated O chondrites are classified into two types, I and II, on the basis of their compositional range. As shown in the Si-(Mg+Fe)-Al diagram (Fig. 10), the matrices of ALH-764 and Y-74191 chondrites are plotted along the tie line connecting olivine and albite, and are grouped into type I. On the other hand,

Table 1. Chemical compositions of matrices of the ALH-764 (LL3) meteorite.

	1 M22	2 M24	3 M26	4 M28	5 M29	6 M31	7 M33	8 M35	9 M36	10 M38	11 M41	12 M42	13 M44
Na_2O	1.99	3.84	4.26	1.84	2.50	2.07	1.44	1.90	3.51	3.34	2.46	2.65	2.30
MgO	18.32	16.60	17.90	13.84	16.38	19.00	23.06	15.01	18.26	17.54	18.95	20.15	20.12
Al_2O_3	3.49	6.78	8.62	3.49	4.50	3.97	2.50	3.91	5.87	6.48	4.27	4.34	4.07
SiO_2	40.43	45.52	48.67	39.51	40.06	38.69	38.50	38.50	42.60	42.82	38.80	38.64	40.45
K_2O	0.31	0.57	1.05	0.34	0.41	0.36	0.21	0.32	0.58	0.51	0.32	0.37	0.28
CaO	1.45	3.21	6.25	2.30	1.31	1.53	0.55	1.99	2.64	2.44	1.60	1.40	1.96
Cr_2O_3	0.10	0.40	0.29	0.33	0.16	0.36	0.25	0.30	0.37	0.29	0.26	0.33	0.37
MnO	0.59	0.43	0.24	0.61	0.71	0.71	0.57	0.58	0.49	0.53	0.56	0.49	0.61
∑FeO	33.37	21.46	12.11	36.31	33.18	31.36	31.57	35.23	23.37	24.51	31.41	30.81	28.38
∑NiO	0.49	0.15	0.64	0.37	0.72	0.58	0.09	0.17	0.13	0.17	0.87	1.26	1.34
S	+	+	+	+	+	+	+	+	+	+	++	++	++
C	+	+	+	+	+	+	+	+	+	+	+	+	+
Total	100.53	98.97	100.03	98.95	99.93	98.62	98.99	97.93	100.82	98.63	99.50	100.43	99.87

	14 M47	15 M49	16 M53	17 M54	18 M56	19 M58	20 M60	21 M62	22 M63	23 M64	24 M65	25 M66	26 M67
Na_2O	3.42	3.08	2.34	2.21	3.29	2.21	1.54	1.03	2.82	2.75	2.58	3.40	2.43
MgO	15.11	16.15	16.12	15.05	15.40	13.33	21.86	28.36	17.04	15.10	18.52	17.60	19.11
Al_2O_3	5.54	6.09	4.38	3.71	5.77	4.27	2.69	2.18	4.47	4.93	4.45	6.69	4.70
SiO_2	41.30	41.31	39.04	36.64	40.43	38.02	37.74	41.26	39.23	36.94	37.92	39.99	39.40
K_2O	0.48	0.57	0.38	0.34	0.54	0.33	0.23	0.19	0.32	0.34	0.37	0.31	0.38
CaO	3.34	2.55	1.99	1.06	2.19	2.93	3.46	1.65	2.41	1.05	1.42	2.21	1.05
Cr_2O_3	0.33	0.29	0.08	0.26	0.20	0.08	0.26	0.53	0.26	0.33	0.39	0.23	0.22
MnO	0.33	0.43	0.57	0.68	0.38	0.61	0.36	0.41	0.50	0.53	0.50	0.37	0.54
∑FeO	26.88	27.37	33.66	36.73	28.67	35.22	29.10	20.49	30.26	35.10	31.19	26.12	29.70
∑NiO	0.32	0.38	0.25	0.40	0.12	0.50	0.15	—	—	—	—	0.40	0.29
S	+	+	+	+	+	+	+	—	—	—	—	+	+
C	+	+	+	+	++	+	+	—	—	—	—	++	+
Total	97.05	98.20	98.82	97.08	96.99	97.51	97.39	96.11	97.31	97.07	97.34	97.32	97.82

+: 0–0.5 (wt%). ++: 0.5–1.0. +++: 1.0–1.5. —: not determined.
∑FeO or ∑NiO mean total Fe or Ni contents as FeO or NiO, respectively.

Table 2. Chemical compositions of matrices of the Y-74191 (L3) meteorite.

	1 M3	2 M5	3 M6	4 M7	5 M11	6 M12	7 M13	8 M14	9 M15	10 M30	11 M17	12 M19	13 M21	14 M23	15 M25
Na_2O	2.73	1.26	1.14	0.59	1.59	2.45	2.48	1.75	2.30	3.51	1.31	1.32	1.38	1.32	1.49
MgO	27.25	28.62	29.68	35.84	26.88	27.02	25.39	23.81	26.80	26.01	31.21	28.48	26.61	30.63	28.25
Al_2O_3	5.51	3.32	2.96	1.13	3.79	5.70	5.32	4.75	4.62	6.42	2.67	2.99	2.86	2.68	3.43
SiO_2	43.66	42.31	40.15	37.48	41.93	43.93	43.39	45.00	42.07	43.60	39.90	42.56	38.79	40.10	42.52
K_2O	0.73	0.85	0.56	0.08	0.70	0.86	0.62	0.26	0.79	0.89	0.43	0.64	0.43	0.61	0.73
CaO	0.88	0.50	0.87	0.24	1.12	0.41	0.76	7.91	0.37	0.52	0.47	0.84	1.90	0.35	0.56
Cr_2O_3	0.90	0.74	0.93	0.65	0.88	0.47	0.53	0.43	0.75	0.37	1.11	0.60	0.52	1.37	0.79
MnO	0.28	0.32	0.45	0.44	0.38	0.36	0.32	0.39	0.43	0.41	0.45	0.32	0.47	0.44	0.49
ΣFeO	15.86	17.84	19.82	21.60	17.52	15.39	17.87	11.41	17.08	16.21	20.56	17.51	21.28	18.53	16.36
ΣNiO	—	—	—	—	0.82	0.19	0.40	0.15	0.30	0.02	0.28	0.17	0.34	0.05	0.04
S	—	—	—	—	+	+	+	+	+	+	+	+	+	+	+
C	—	—	—	—	+	+	+	+	+	+	+	+	+	+	++
Total	97.79	95.75	96.56	98.06	95.60	96.78	97.08	95.88	95.50	97.96	98.37	95.44	94.58	96.09	94.66

Table 3. Chemical compositions of matrices of the ALH-77015 (L3) meteorite.

	1 M20	2 M21	3 M22	4 M23	5 M25	6 M26	7 M30	8 M31	9 M32	10 M33
Na_2O	0.30	0.20	0.26	0.16	0.20	0.19	0.48	0.14	0.35	0.50
MgO	19.54	23.76	23.57	22.93	21.36	23.03	22.77	24.93	22.08	19.75
Al_2O_3	1.85	1.59	1.47	1.54	1.71	1.35	2.63	1.20	1.25	2.39
SiO_2	27.15	32.71	34.48	27.44	31.50	28.85	33.37	34.73	29.55	32.00
K_2O	0.01	0.02	0.05	0.02	0.01	0.01	0.07	0.01	0.04	0.08
CaO	0.12	0.56	1.70	0.21	0.44	0.85	0.88	0.32	0.56	1.11
Cr_2O_3	0.63	0.58	0.51	0.47	0.47	0.43	0.68	0.79	0.66	0.40
MnO	0.42	0.56	0.44	0.39	0.53	0.40	0.48	0.58	0.49	0.52
ΣFeO	39.04	31.85	29.47	33.54	33.76	30.64	31.54	36.78	34.42	33.16
ΣNiO	1.54	1.04	0.48	1.47	0.66	2.15	1.12	0.41	0.96	1.83
S	++	+	+	+	++	+	+	+	+	+
C	++	+	+	+++	+	++	+	+	++	++
Total	90.58	92.87	92.42	88.17	90.64	87.91	94.01	99.90	90.31	91.73

	11 M35	12 M36	13 M37	14 M38	15 72′-1M	16 72′-2M	17 2M	18 11-1	19 11-2	20 5M
Na_2O	0.36	0.28	0.66	0.17	0.11	0.25	0.95	0.25	0.60	0.18
MgO	20.31	22.66	21.88	23.19	17.80	24.10	21.83	21.74	22.63	20.80
Al_2O_3	1.87	1.82	1.93	1.43	1.72	2.10	2.52	1.61	1.66	1.51
SiO_2	30.07	31.69	29.00	30.29	25.81	31.55	36.18	34.53	31.28	33.01
K_2O	0.02	0.02	0.00	0.01	0.03	0.06	0.12	0.01	0.09	0.03
CaO	0.74	0.66	1.23	0.75	0.10	0.36	0.91	0.74	1.04	0.34
Cr_2O_3	0.57	0.50	0.46	0.56	0.58	0.60	0.75	0.82	0.74	0.42
MnO	0.50	0.55	0.35	0.42	0.31	0.29	0.36	0.56	0.27	0.40
ΣFeO	34.65	33.29	31.08	31.58	41.33	29.97	30.98	34.32	34.38	37.46
ΣNiO	1.58	1.26	2.06	1.71						
S	+	+	+	+						
C	++	+	++	++						
Total	90.66	92.74	88.65	90.10	87.79	89.29	94.60	94.56	92.68	94.16

the matrices of ALH-77015, ALH-77033 and ALH-77249 chondrites cluster nearly parallel to the (Mg+Fe)-Si side line just above the olivine-albite join as shown in Fig. 10b. They define the type II matrix. The matrix of ALH-77003 chondrite belongs to type II. The matrices of ALH-77299 chondrite are plotted in SiO_2-rich area as shown in Fig. 10a and are conveniently classified as type I′. These matrices are considered to be a mixture of the type I matrix and fine-grained mineral fragments as mentioned in the previous section.

Table 4. Chemical compositions of matrices of the ALH-77033 (L3) meteorite.

	1 M1	2 M2	3 M3	4 M4	5 M5	6 M6	7 M7	8 M8	9 M9	10 M10	11 KM1	12 KM2	13 KM3	14 KM4
Na_2O	0.59	0.12	0.20	0.95	1.00	0.20	0.20	0.31	0.13	0.16	0.20	0.09	0.23	1.29
MgO	26.88	19.37	24.10	20.08	25.08	26.93	22.46	22.13	21.42	22.15	23.80	21.30	23.36	22.28
Al_2O_3	1.59	1.49	1.50	2.67	2.32	1.63	1.16	1.77	1.48	1.15	1.57	2.24	2.20	3.51
SiO_2	32.31	26.35	28.97	33.96	33.41	34.98	27.48	30.98	28.87	29.96	31.51	32.53	32.51	34.21
K_2O	0.09	0.05	0.03	0.13	0.10	0.04	0.04	0.07	0.04	0.03	0.05	0.03	0.02	0.30
CaO	0.20	0.18	0.27	3.14	2.26	0.59	0.03	0.57	0.43	0.24	0.40	1.63	0.44	1.70
TiO_2	—	—	—	—	—	—	—	—	—	—	0.02	0.06	0.08	0.12
Cr_2O_3	0.60	0.60	0.50	0.65	0.52	0.75	0.51	0.49	0.28	0.56	0.83	0.52	0.59	0.59
MnO	0.55	0.54	0.49	0.64	0.55	0.54	0.35	0.52	0.42	0.44	0.33	0.28	0.44	0.40
ΣFeO	32.18	37.58	33.12	26.35	25.76	27.09	36.17	36.49	35.01	33.18	34.21	34.89	34.85	31.35
ΣNiO	—	—	—	—	—	—	—	—	—	—	1.37	1.21	1.16	1.30
Total	94.99	86.27	89.16	88.56	91.00	92.75	88.40	93.32	88.07	87.87	94.29	94.77	95.87	97.04

	15 KM5	16 KM6	17 KM7	18 KM8	19 KM9	20 KM10	21 KM11	22 KM12	23 KM13	24 KM14	25 KM15	26 KM16	27 KM17	28 KM18
Na_2O	0.13	0.02	0.27	0.21	0.75	0.14	0.04	0.15	0.16	0.11	0.14	0.81	0.13	0.21
MgO	23.55	27.88	23.71	25.64	26.17	24.76	29.82	24.58	23.29	24.98	27.51	23.92	18.37	21.91
Al_2O_3	1.43	0.14	3.14	2.52	3.05	2.52	1.37	1.54	1.76	0.77	1.59	2.42	1.95	2.36
SiO_2	34.77	34.51	29.41	35.49	35.26	33.30	35.73	32.54	33.46	33.56	38.71	31.71	29.02	29.24
K_2O	0.01	0.01	0.02	0.09	0.22	0.03	0.01	0.03	0.05	0.00	0.03	0.02	0.04	0.03
CaO	0.20	0.05	0.65	0.44	1.08	0.14	0.53	0.55	0.62	0.29	0.43	0.33	0.28	0.17
TiO_2	0.04	0.04	0.22	0.16	0.08	0.09	0.06	0.09	0.07	0.04	0.06	0.10	0.13	0.15
Cr_2O_3	0.56	0.14	8.03	0.59	0.94	0.33	0.41	1.05	0.66	0.16	0.48	0.42	0.31	0.67
MnO	0.35	0.58	0.55	0.44	0.30	0.36	0.48	0.44	0.54	0.61	0.57	0.43	0.41	0.38
ΣFeO	32.99	37.77	31.53	29.97	28.55	31.76	30.64	34.05	35.11	34.93	29.56	34.61	39.94	37.41
ΣNiO	2.40	0.26	1.13	0.60	0.71	2.49	0.31	1.59	1.12	0.72	0.47	2.51	1.40	2.19
Total	96.44	101.39	98.64	96.13	97.11	95.92	99.41	96.61	96.82	96.16	99.54	96.56	91.97	94.74

Table 5. Chemical compositions of matrices of the ALH-77003 (L3 or C3) meteorite.

	1 KM1	2 KM2	3 KM3	4 KM4	5 KM5	6 KM6	7 KM7	8 KM8	9 KM9	10 KM10	11 KM11	12 KM12	13 KM13
Na_2O	0.15	0.18	0.12	0.21	0.16	0.18	0.18	0.23	0.11	0.17	0.42	0.20	0.15
MgO	26.11	24.88	26.61	25.63	29.00	27.85	26.83	23.13	26.57	24.99	26.12	25.73	24.39
Al_2O_3	2.26	1.15	1.13	1.84	2.53	2.33	0.60	1.57	2.87	2.54	1.46	1.49	1.25
SiO_2	31.30	29.14	30.34	30.84	32.26	32.61	32.11	29.53	32.37	31.00	35.40	31.80	28.08
K_2O	0.03	0.02	0.03	0.05	0.02	0.04	0.05	0.07	0.04	0.03	0.07	0.06	0.07
CaO	0.09	0.29	0.07	0.11	0.12	0.08	0.36	1.26	0.13	0.12	1.73	0.28	0.10
TiO_2	0.11	0.04	0.06	0.06	0.12	0.11	0.03	0.06	0.07	0.08	0.02	0.12	0.06
Cr_2O_3	0.32	0.32	0.27	0.45	0.40	0.53	0.41	0.22	0.64	0.63	0.26	0.47	0.30
MnO	0.35	0.31	0.24	0.35	0.30	0.36	0.29	0.24	0.29	0.38	0.33	0.25	0.21
ΣFeO	30.85	39.62	36.04	35.96	30.89	30.79	36.74	37.07	31.77	32.54	32.23	36.20	39.88
ΣNiO	0.63	0.32	0.91	0.98	1.22	0.27	0.73	0.97	0.39	0.59	0.83	0.34	1.27
Total	92.19	96.24	95.81	96.47	97.03	95.13	98.33	94.33	95.23	93.06	98.85	96.94	95.76

	14 KM14	15 KM15	16 KM16	17 KM17	18 KM18	19 KM19	20 KM20	21 KM21	22 KM22	23 KM23	24 KM24	25 KM25	26 KM26
Na_2O	0.21	0.15	0.12	0.22	0.15	0.15	0.46	0.30	0.13	0.31	0.21	0.09	0.67
MgO	25.99	28.78	28.30	25.14	25.21	25.68	22.99	22.99	26.36	25.01	29.94	23.82	22.49
Al_2O_3	2.73	1.66	0.61	2.04	1.41	1.37	1.74	1.11	1.92	1.72	1.62	1.23	3.57
SiO_2	31.55	32.65	35.72	29.24	30.04	29.53	28.28	27.71	30.67	31.48	30.31	27.80	27.59
K_2O	0.06	0.03	0.03	0.04	0.05	0.03	0.09	0.06	0.02	0.06	0.08	0.00	0.12
CaO	0.09	0.20	1.82	0.23	0.12	0.11	0.30	0.13	0.10	0.24	0.32	0.09	0.34
TiO_2	0.05	0.17	0.10	0.08	0.13	0.08	0.07	0.04	0.03	0.09	0.08	0.05	0.07
Cr_2O_3	0.60	0.37	0.27	0.45	0.46	0.30	0.29	0.38	0.41	0.46	0.27	0.18	0.52
MnO	0.43	0.30	0.28	0.27	0.38	0.17	0.34	0.29	0.28	0.28	0.29	0.00	0.29
ΣFeO	33.86	31.90	31.98	37.62	35.75	36.77	39.21	40.68	37.33	38.27	36.50	39.35	36.87
ΣNiO	1.44	0.98	0.34	0.45	1.97	2.06	1.30	0.67	0.46	0.67	0.74	2.13	2.46
Total	96.99	97.17	99.57	95.76	95.66	96.25	95.07	94.34	97.71	98.57	95.36	94.76	94.99

Table 6. Chemical compositions of matrices of the ALH-77249 (L3) meteorite.

	1 KM1	2 KM2	3 KM3	4 KM4	5 KM5	6 KM6	7 KM7	8 KM8	9 KM9	10 KM10	11 KM11	12 KM12
Na_2O	0.15	0.20	0.09	0.14	0.19	0.21	0.20	0.28	0.18	0.02	0.10	0.41
MgO	28.23	19.84	23.07	21.60	24.03	21.34	18.95	19.75	18.48	22.62	19.00	25.65
Al_2O_3	1.32	1.69	1.51	1.24	2.38	1.43	2.77	3.00	1.15	1.11	1.48	2.93
SiO_2	34.90	28.71	31.29	28.83	36.19	29.56	30.50	30.10	29.81	27.30	28.53	34.10
K_2O	0.05	0.03	0.00	0.02	0.07	0.03	0.13	0.13	0.03	0.02	0.01	0.05
CaO	1.03	0.26	0.03	0.09	0.46	0.25	0.23	0.26	0.28	0.11	0.39	0.60
TiO_2	0.03	0.06	0.07	0.02	0.12	0.08	0.10	0.13	0.05	0.03	0.09	0.12
Cr_2O_3	0.80	0.42	0.51	0.34	0.60	0.60	0.52	0.84	0.46	0.18	0.49	0.53
MnO	0.46	0.52	0.47	0.40	0.38	0.50	0.48	0.36	0.33	0.30	0.36	0.44
ΣFeO	30.06	40.89	37.95	38.52	31.09	39.93	39.31	39.25	40.86	40.20	39.58	31.73
ΣNiO	0.72	1.83	1.26	1.55	1.62	1.50	1.15	1.34	0.98	2.00	3.52	1.79
Total	97.76	94.47	96.24	92.75	97.13	95.42	94.34	95.44	92.60	93.90	93.54	98.33

	13 KM13	14 KM14	15 KM15	16 KM16	17 KM17	18 KM18	19 KM19	20 KM20	21 KM21	22 KM22	23 KM23
Na_2O	0.13	0.10	0.12	0.25	0.38	0.23	0.12	0.08	0.33	0.22	0.20
MgO	16.78	19.52	17.26	16.76	23.47	22.69	23.46	18.80	19.31	21.36	22.22
Al_2O_3	3.07	0.83	1.32	1.37	1.09	1.40	1.04	1.90	1.17	1.52	1.73
SiO_2	23.69	28.78	26.01	24.67	33.69	34.06	32.64	26.09	28.81	32.81	30.68
K_2O	0.05	0.03	0.03	0.09	0.08	0.08	0.01	0.06	0.05	0.05	0.17
CaO	0.11	0.11	0.22	0.53	0.20	0.29	0.11	0.21	0.77	1.08	0.22
TiO_2	0.00	0.04	0.07	0.06	0.04	0.07	0.04	0.09	0.08	0.08	0.04
Cr_2O_3	0.42	0.30	0.36	0.69	0.39	0.44	0.48	2.15	0.50	0.60	0.51
MnO	0.32	0.48	0.36	0.43	0.62	0.50	0.55	0.47	0.39	0.36	0.43
ΣFeO	43.57	43.03	41.75	39.21	37.85	37.43	38.07	42.36	38.91	35.13	13.30
ΣNiO	2.96	1.68	4.43	1.93	0.37	0.19	1.04	0.53	2.21	2.05	1.57
Total	91.08	94.90	91.92	86.00	98.18	97.36	97.56	92.73	92.51	95.25	94.05

Table 7. Chemical compositions of matrices of the ALH-77299 (H3) meteorite.

	1 25M	2 141M	3 M3	4 M4	5 M5	6 M6	7 M8	8 M10
Na_2O	2.61	1.48	2.01	1.70	0.96	2.94	2.51	1.00
MgO	25.20	29.42	24.15	26.43	26.54	24.13	15.00	17.18
Al_2O_3	4.53	2.26	3.01	3.37	1.80	4.68	4.11	1.82
SiO_2	47.67	38.81	41.69	42.68	48.71	41.42	46.67	46.84
K_2O	0.30	0.07	0.35	1.13	0.19	0.16	0.47	0.74
CaO	3.69	1.08	1.05	1.12	0.61	1.65	5.05	2.02
Cr_2O_3	0.67	0.67	—	—	—	—	—	—
MnO	0.43	0.37	0.50	0.45	0.42	0.45	0.53	0.89
ΣFeO	15.12	22.92	24.66	23.70	18.02	24.24	20.84	27.65
Total	100.22	97.09	97.41	100.58	97.24	99.67	95.17	98.14

4.1. *Type I matrix*

As shown in Fig. 7a and 8a, the (Na+K)/Al ratios of the type I matrix are close to unity. This indicates that Na and Al construct the normative components of albite, nepheline or jadite in the matrix. On the other hand, Si-(Mg+Fe)-Al plotting (Fig. 10a) indicates that most Al contents of the type I matrix form albite molecule together with the Si content. Furthermore, the type I matrix is almost lacking in Ca-poor pyroxene component. Figure 9a shows the normative olivine component to be rich in fayalite. As shown in Fig. 8a, small amounts of Ca-bearing phases such as Ca-rich pyroxene, Ca-phosphates or Ca-carbonate must exist in the matrix. The type I matrix then consists mainly of the normative components of ferrous olivine and sodic plagioclase with small amounts of Ca-bearing phases.

The actual minerals occurring in the type I matrix were identified by using STEM for submicroscopic grains less than about 0.5 microns. They are ferrous olivine

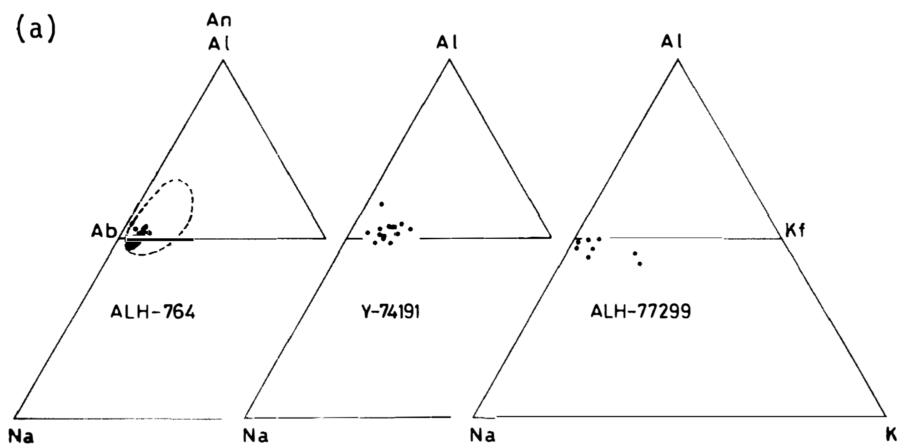

Fig. 7.

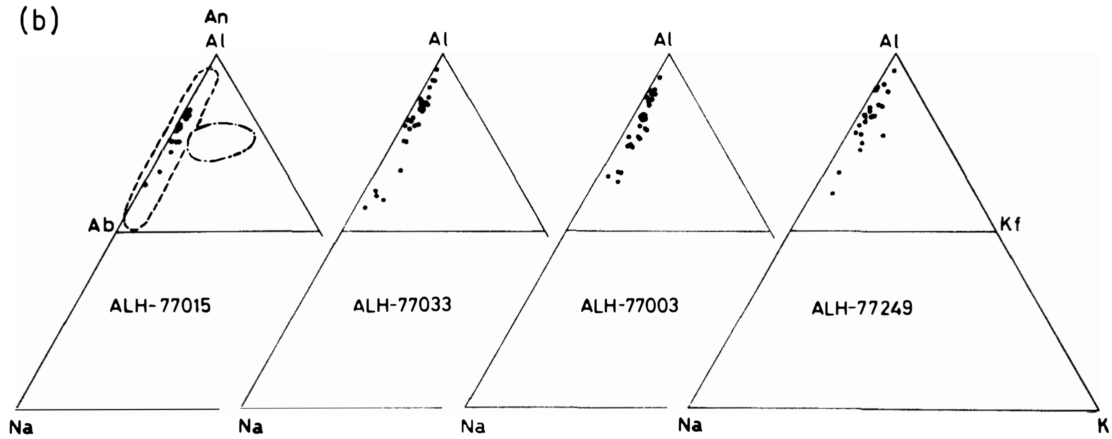

Fig. 7. Atomic ratios of Na, K and Al of the matrices. An, Ab and Kf mean anorthite, albite and K-feldspar components, respectively. The area by bar curve in Fig. 7a is the compositional range of the matrices of unequlibrated O chondrites reported by HUSS *et al. (1981). The areas by dot-bar curve and bar curve in Fig. 7b are the compositional ranges of the matrices of CI chondrites and C2 and C3 chondrites reported by* MCSWEEN *and* RICHARDSON *(1977), respectively.*

($Fo_{60-50}Fa_{40-50}$), Ca-rich pyroxene, whitlockite, nickeliferous Fe-metal ($Fe_{50}Ni_{50}$), chromite, troilite, limonite, amorphous material and so on. The limonite occurs as veins in association with large Fe-metal or troilite grains and may be a product of alteration. The amorphous material and ferrous olivine are the most abundant constituents of the type I matrix. The former is glass including variable amount of small spherical grains of nickeliferous Fe-metal about 0.01 to 0.1 microns in size (Fig. 11). The chemical composition of the glass is represented by a mixture of albite (or sodic plagioclase) and ferrous olivine. The mixing ratio varies and some parts of the glass are nearly equal to albite in chemical composition, but other parts are rich in ferrous olivine components of about $Fo_{50}Fa_{50}$.

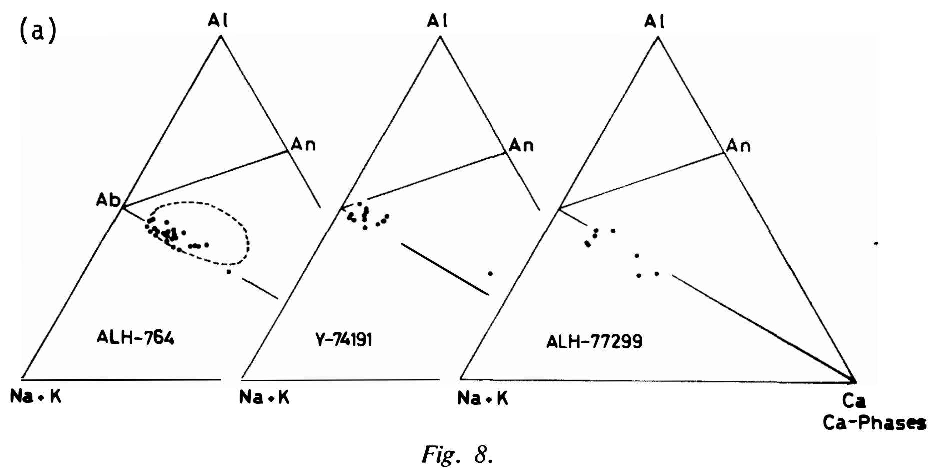

Fig. 8.

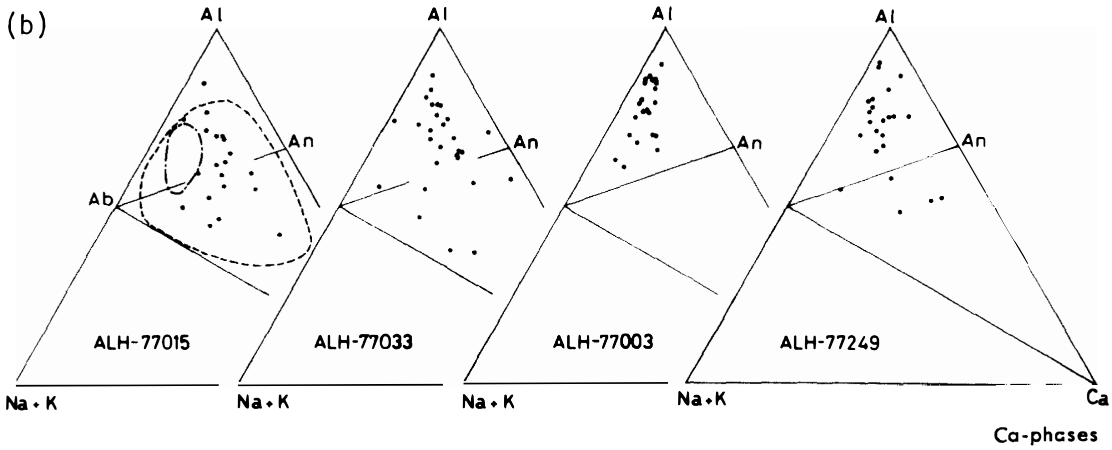

Fig. 8. Atomic ratios of Al, (Na+K) and Ca of the matrices. Abbreviation and the curves are the same as those in Fig. 7. Ca-phases mean the component of Ca-bearing minerals such as Ca-rich pyroxene, whitlockite, apatite, calcite, etc.

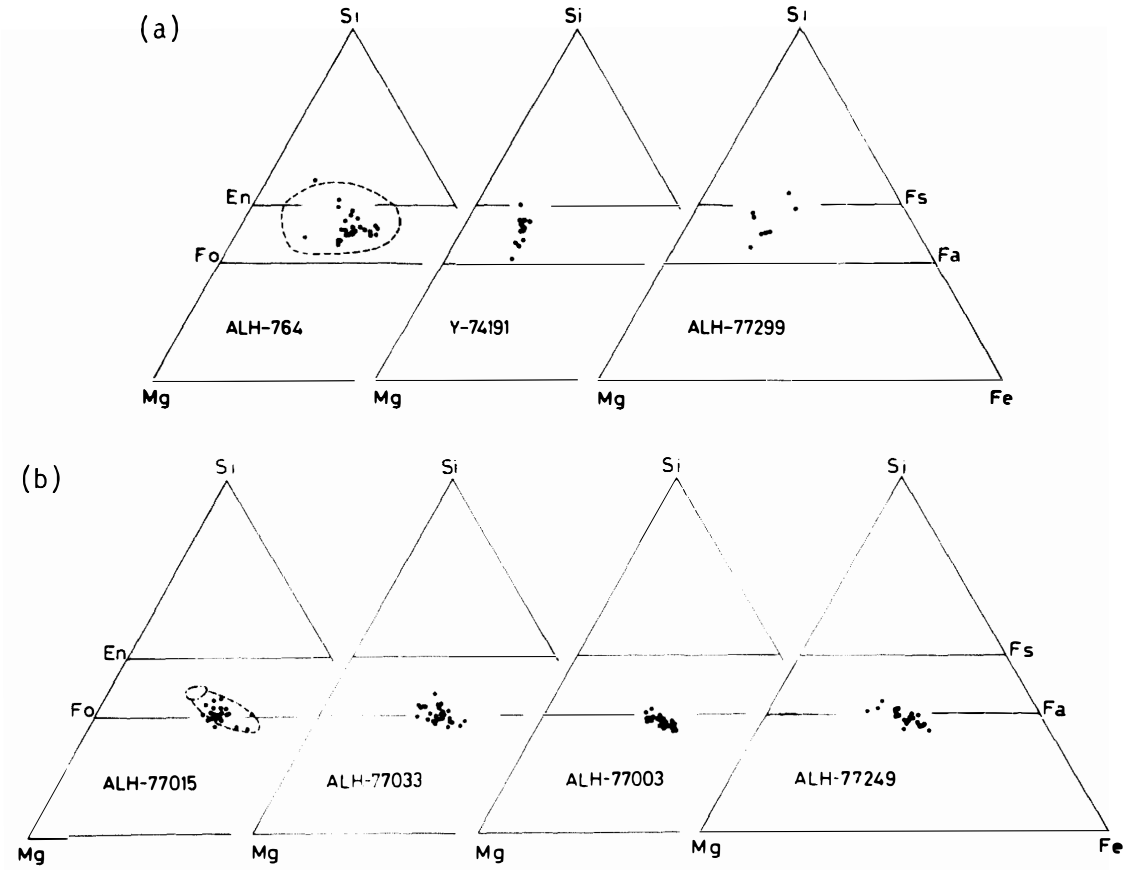

Fig. 9. Atomic ratios of Si, Mg and Fe of the matrices. En, Fs, Fo and Fa are enstatite, ferrosilite, forsterite and fayalite components, respectively. The curves are the same as in Fig. 7.

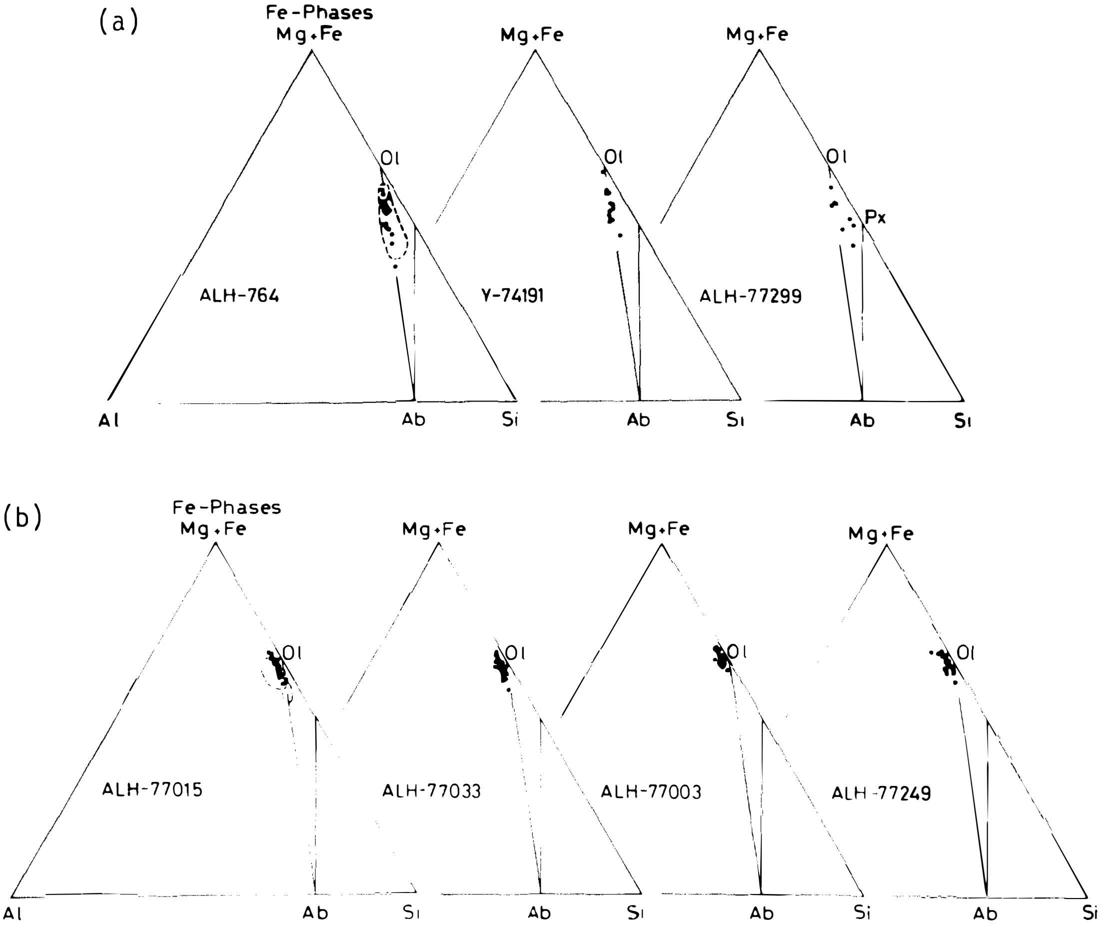

Fig. 10. Atomic ratios of Si, (Mg+Fe) and Al of the matrices. Ol, Px, Ab and Fe-phases mean the components of olivine, Ca-poor pyroxene, albite and Fe-bearing minerals such as Fe-metal, troilite, magnetite, limonite, etc., respectively. The curves are the same as in Fig. 7.

4.2. *Type II matrix*

The type II matrices are relatively homogeneous in chemical composition except for the alkali components and are almost the same as the matrices of carbonaceous chondrites of types C2 and C3 (McSWEEN and RICHARDSON, 1977) as shown in Figs. 7b, 8b, 9b and 10b. They show remarkable differences from the type I matrix in the (Na+K)/Al ratio. The ratios of the type II matrix are less than unity and are variable, whereas those of the type I matrix are nearly close to unity. This means there is a deficiency of the Na content with respect to Al in the type II matrices. The type II matrices are plotted showing a wide range of the Al-(Na+K)-Ca ratio and no connection with the plagioclase (Fig. 8b), indicating that plagioclase became unstable prior to or after the matrix formation.

According to STEM, submicroscopic grains in the type II matrix of ALH-77015

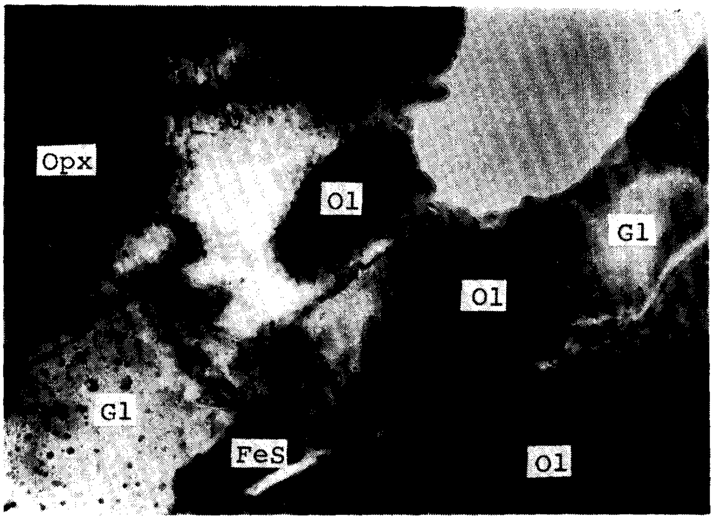

Fig. 11. Matrix of ALH-764 chondrite by transparent electron microscopy. Glass (Gl) occurs as "glue" which fills the interstitial spaces between large or fine crystal grains of olivine (Ol), troilite (FeS), Ca-poor pyroxene (Opx), etc. The Ca-poor pyroxene is large crystal fragment and not matrix mineral. Long dimension is about 2 microns.

Fig. 12. Matrix of ALH-77015 chondrite by transparent electron microscopy. This figure is a portion of large glass which occurs between chondrules or large mineral fragments. Long dimension is about 2 microns.

chondrite are olivine, Ca-rich pyroxene, troilite, pentlandite, Fe-phase (magnetite?), limonite, amorphous material and so on. The amorphous material is glass and is the main constituent of the matrix (Fig. 12). It is free from fine grains such as Fe-metal observed in the amorphous material of the type I matrix. The chemical composition of glass is close to those of bulk matrices except that the former is slightly enriched in Si and Al.

5. Discussion

The matrices of carbonaceous chondrites (McSWEEN and RICHARDSON, 1977) are shown in Figs. 7b, 8b, 9b and 10b. The matrices of Cl chondrites are different in chemical composition from those of C2 and C3 chondrites. However, the bulk composition of Cl chondrites is nearly the same as those of the matrices of C2 and C3 chondrites. This means that the matrices of Cl chondrites are represented by the composition which might result by the subtraction of Fe-phases such as magnetite from the bulk composition by low-temperature mineralization (KERRIDGE *et al.*, 1979). On the other hand, the matrices of unequilibrated O chondrites reported by HUSS *et al.* (1981) are distinctly different from those of C_2 and C3 chondrites as shown in Figs. 7, 8, 9 and 10.

In this paper, the matrices of unequilibrated O chondrites are classified into type I and type II, the former corresponding to those reported by HUSS *et al.* (1981), and the latter to those of C2 and C3 chondrites.

The main difference in composition between them is that, as already stated, the type II matrices show a deficiency of Na contents with respect to Al and the instability or decomposition of plagioclase prior to or after the matrix formation. According to "prior to" and "after", two possibilities are considered for these natures of the type II matrices.

One possibility is that the type II matrices included originally Na, Al and Ca as variable amounts of nepheline (and/or albite), Al-bearing phases such as spinels, and Ca-bearing phases. The nepheline component may be produced prior to the matrix formation in the primitive nebula including albite and Fe-metal by the following equation:

$$\underset{\text{albite}}{NaSi_3AlO_8} + \underset{\text{metal}}{4Fe} + \underset{\text{gas}}{2O_2} = \underset{\text{nepheline}}{NaSiAlO_4} + \underset{\text{olivine}}{2Fe_2SiO_4}.$$

The other is the alteration after the matrix formation on a parental body with the partial loss of alkali contents from the matrix which was originally comprised of Na and Al as sodic plagioclase component.

Recently BUNCH and CHANG (1980) discussed the matrices of C2 chondrites and concluded that they were formed through hydrothermal alteration in the parent body, resulting in partial loss of Na with addition of H_2O and CO_2. It is unknown whether this is a valid explanation for the type II matrices of O chondrites or not, but variable amounts of Na may have been lost from the original matrix which had contained more Na as a sodic plagioclase component.

Thus, the original material of the type II matrices may be a mixture of normative components of ferrous olivine, sodic plagioclase (or nepheline and Al-bearing phases) and Fe-phases with small amounts of Ca-bearing phases. The sodic plagioclase component if present is considered to have formed a glass with ferrous olivine component after the partial loss of alkali contents. The olivine component occurs as both fine olivine grains and a component of the glass. The Fe-phases are Fe-Ni metal, troilite and their altered products. Ca-bearing phases are Ca-rich pyroxene, whitlockite and calcite.

On the other hand, the type I matrices include enough Na to form sodic plagioclase component, and are not considered to suffer from any loss of alkali content. They consist of ferrous olivine and sodic plagioclase components with small amounts of Ca-bearing phases and Fe-Ni metal. Thus, the main constituents of the type I matrices resemble those of the original type II matrices, but are different in the mixing ratios of each other. Namely, the type I matrices contain high and variable amounts of sodic plagioclase component, and the type II contains lower and constant amounts of sodic plagioclase (or nepheline and Al-bearing phases) and higher amounts of Fe-phases.

The occurrence of amorphous materials in unequilibrated chondrites has not been adequately clarified (ASHWORTH, 1977; BUNCH and CHANG, 1980; HUSS *et al.*, 1981). The amorphous materials seem to be a main constituent of most of the chondrites reported in this paper (Figs. 11 and 12). The amorphous material is massive as observed from the image of the transparent electron microscope (TEM) and shows no evidence of crystallographic outline, cleavage, twinning and diffraction pattern of transparent electrons. Thus, it is mainly glass which cements the very fine grains of the matrices as "glue". The origin of the glass is not known but it may be explained by shock events which produced a melt from extremely fine-grained substances consisting of ferrous olivine and sodic plagioclase for the type I matrix and consisting of the already alkali-depleted material for the type II matrix. The grains of ferrous olivine, troilite, Ca-phosphates, pyroxenes, metal, etc., which occur in the matrix and are larger than an order of 0.1 microns, are considered to have been too large to be melted by the shock events. As stated in the foregoing section, the glass in the matrices of ALH-764 chondrite includes small spherules of Fe-Ni metal less than 0.1 microns in size (Fig. 11). This may be due to liquid immiscibility which then supports the shock-melt origin for the matrix glass.

The chemical compositions of the major bulk chondrules are decidedly different from those of their matrices. In general, the matrices are rich in FeO and poor in SiO_2. The SiO_2-rich nature of the chondrules results in an abundant occurrence of Ca-poor pyroxene and/or SiO_2-rich groundmass in the droplet chondrules, even though the Ca-poor pyroxene component is absent in most matrices. The type I′ matrices are comprised of abundant fine fragments of Ca-poor pyroxene which may be derived from broken chondrules or lithic fragments, and apparently show the SiO_2-rich nature of the type I′.

The "dark clasts" are a kind of lithic fragment and rarely occur in unequilibrated chondrites. They consist of opaque minerals and matrix-like materials which are slightly darker than the normal matrix surrounding the dark clasts (Fig. 2). The opaque minerals are troilite and Fe-metal whose grain size ranges from several to

Table 8. Chemical compositions of dark clasts of the ALH-764 (LL3) meteorite.

	1 617A	2 617B	3 599-1	4 599-2
Na_2O	1.40	1.22	0.89	0.97
MgO	24.58	23.71	23.85	21.83
Al_2O_3	3.06	2.73	2.22	2.14
SiO_2	37.52	37.68	38.18	37.98
K_2O	0.20	0.18	0.16	0.21
CaO	0.96	1.77	1.42	2.25
Cr_2O_3	0.55	0.48	0.41	0.36
MnO	0.58	0.57	0.40	0.35
ΣFeO	30.12	31.10	28.42	29.17
ΣNiO	1.04	0.80	0.71	0.60
S	++	++	+	+
C	+	+	++	++
Total	100.01	100.25	96.66	95.85

+, ++: the same as in Table 1.

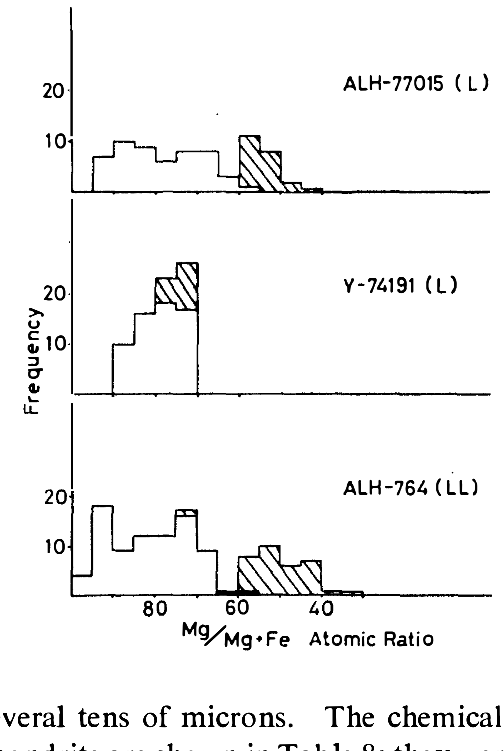

Fig. 13. Frequency diagrams of Mg×100/(Mg+Fe) of chondrules (blank area), dark clasts (black area) and matrices (shaded area).

several tens of microns. The chemical compositions of the dark clasts of ALH-764 chondrite are shown in Table 8; they were obtained by the same method as the matrices. The chemical compositions of the dark clasts correspond to just the join-point between the compositional ranges of chondrules and matrices. The main-type chondrules (SP-chondrules of IKEDA (1980)) range from a pyroxene-rich composition to an olivine-rich composition with nearly constant amounts of sodic plagioclase The olivine-rich composition, which is roughly represented by a mixture of olivine and sodic plagioclase in the ratio of about 10: 1, is nearly equal to the chemical composition of the dark clasts, which in turn corresponds to the plagioclase-poor matrices. As shown in Fig. 13, the Mg/(Mg+Fe) ratios of the dark clasts also show the same situation and are plotted between the chondrules and the matrices. These compositional relationships among chondrules, dark clasts and matrices show a continuous spectrum in chemical compositions and suggests strong genetic correlation among them.

The ferrous nature of matrix olivine-components is well represented in Fig. 9b where the type II matrices form a trend along the tie line from En to the Fe apex. Considering the SiO_2 contents due to the normative compositions of plagioclase and Ca-rich pyroxene in the type II matrices, the trend of the type II matrix and probably the C2 matrices suggests that they are mixtures of mainly ferrous olivine (about $Fo_{60-50}Fa_{40-50}$) and Fe-bearing phases such as nickeliferous Fe-metal, troilite, or their alteration products including magnetite. The ferrous olivine composition of about $Fo_{50}Fa_{50}$ is considered to be a result of the reaction in the cooling nebula,

$$\underset{\text{pyroxene}}{MgSiO_3} + \underset{\text{metal}}{Fe} + \underset{\text{gas}}{1/2O_2} = \underset{\text{olivine}}{(Mg_1Fe_1)_2SiO_4} .$$

According to the condensation theory (LARIMER and ANDERS, 1967; GROSSMAN and LARIMER, 1974), this ferrous olivine becomes stable at a temperature lower than about 700 K, and the matrices of unequilibrated O chondrites are considered to represent the low temperature condensate from the primitive nebula.

Acknowledgments

We thank Prof. M. KUBOTA of Ibaraki University, Dr. K. YANAI of the National Institute of Polar Research and Dr. G. SATO of Chiba University for permitting us to use the electron-probe microanalyzers, and we are grateful to Prof. N. ONUMA of Ibaraki University for critical reading of the manuscript.

References

ASHWORTH, J. R. (1977): Matrix textures in unequilibrated ordinary chondrites. Earth Planet. Sci. Lett., **35**, 25–34.

BENCE, A. E. and ALBEE, A. L. (1968): Empirical correction factors for the electron microanalysis of silicates and oxides. J. Geol., **76**, 382–403.

BUNCH, T. E. and CHANG, S. (1980): Carbonaceous chondrites. II. Carbonaceous chondrite phyllosilicates and light element geochemistry as indicators of parent body processes and surface conditions. Geochim. Cosmochim. Acta, **44**, 1543–1577.

DODD, R. T. (1978): The composition and origin of large microporphyritic chondrules in the Manych (L3) chondrite. Earth Planet. Sci. Lett., **39**, 52–66.

FODER, R. V. and KEIL, K. (1978): Catalog of lithic fragments in LL-group chondrites. Univ. New Mexico, Inst. Meteoritics, Spec. Pub., No. 19.

GROSSMAN, L. and LARIMER, J. W. (1974): Early chemical history of the solar system. Rev. Geophys. Space Phys., **12**, 71–101.

HUSS, G. R., KEIL, K. and TAYLOR, G. J. (1981): The matrices of unequilibrated ordinary chondrites: Implications for the origin and history of chondrites. Geochim. Cosmochim. Acta, **45**, 33–51.

IKEDA, Y. (1980): Petrology of Allan Hills-764 chondrite (LL3). Mem. Natl Inst. Polar Res., Spec. Issue, **17**, 50–82.

IKEDA, Y. and TAKEDA, H. (1979): Petrology of the Yamato-74191 chondrite. Mem. Natl Inst. Polar Res., Spec. Issue, **12**, 38–58.

KERRIDGE, J. F., MACKAY, A. L. and BOYNTON, W. V. (1979): Magnetite in CI carbonaceous meteorites: Origin by aquaous activity on a planetesimal surface. Science, **205**, 395–397.

KIMURA, M., YAGI, K. and ONUMA, K. (1979): Petrological studies on chondrules in Yamato-74 meteorites. Mem. Natl Inst. Polar Res., Spec. Issue, **12**, 114–133.

LARIMER, J. W. and ANDERS, E. (1967): Chemical fractions in meteorites-II. Abundance patterns and their interpretation. Geochim. Cosmochim. Acta, **31**, 1239–1270.

MCSWEEN, H. Y., JR. (1977): Chemical and petrographic constraints on the origin of chondrules and inclusions in carbonaceous chondrites. Geochim. Cosmochim. Acta, **41**, 1843–1860.

MCSWEEN, H. Y., JR. and RICHARDSON, S. M. (1977): The composition of carbonaceous chondritic matrix. Geochim. Cosmochim. Acta, **41**, 1145–1161.

SCORE, R., SCHWARZ, C. W., KING, T. V. V., MASON, B., BOGARD, D. D. and GABEL, E. M. (1981): Antarctic meteorite descriptions 1976–1977–1978–1979. Antarct. Meteorite Newsl., **4**(1), 144 p.

WALTER, L. S. (1969): The major element composition of individual chondrules of the Bjurböle meteorite. Meteorite Research, ed. by P. M. MILLIMAN. Dordrecht, D. Reidel, 191–205.

WALTER, L. S. and DODD, R. T. (1972): Evidence for vapor fractionation in the origin of chondrules. Meteoritics, **7**, 341–352.

(*Received May 23, 1981*)